

Exogenous Gene Integration for Microalgal Cell Transformation Using a Nanowire-Incorporated Microdevice

Sunwoong Bae,[†] Seunghye Park,[‡] Jung Kim,[§] Jong Seob Choi,[†] Kyung Hoon Kim,[†] Donguk Kwon,[§] EonSeon Jin,[‡] Inkyu Park,[§] Do Hyun Kim,[†] and Tae Seok Seo^{*,†}

[†]Department of Chemical and Biomolecular Engineering, Korea Advanced Institute of Science and Technology (KAIST), 291 Daehak-ro, Yuseong-gu, Daejeon 305-701, Republic of Korea

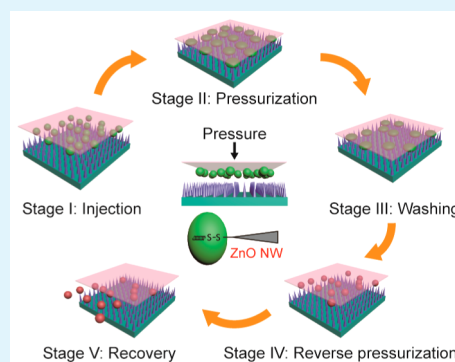
[‡]Department of Life Science, Research Institute for Natural Sciences, Hanyang University, Seoul 133-791, Republic of Korea

[§]School of Mechanical, Aerospace and Systems Engineering, Division of Mechanical Engineering, Korea Advanced Institute of Science and Technology (KAIST), 291 Daehak-ro, Yuseong-gu, Daejeon 305-701, Republic of Korea

S Supporting Information

ABSTRACT: Superior green algal cells showing high lipid production and rapid growth rate are considered as an alternative for the next generation green energy resources. To achieve the biomass based energy generation, transformed microalgae with superlative properties should be developed through genetic engineering. Contrary to the normal cells, microalgae have rigid cell walls, so that target gene delivery into cells is challengeable. In this study, we report a ZnO nanowire-incorporated microdevice for a high throughput microalgal transformation. The proposed microdevice was equipped with not only a ZnO nanowire in the microchannel for gene delivery into cells but also a pneumatic polydimethylsiloxane (PDMS) microvalve to modulate the cellular attachment and detachment from the nanowire. As a model, hygromycin B resistance gene cassette (Hyg3) was functionalized on the hydrothermally grown ZnO nanowires through a disulfide bond and released into green algal cells, *Chlamydomonas reinhardtii*, by reductive cleavage. During Hyg3 gene delivery, a monolithic PDMS membrane was bent down, so that algal cells were pushed down toward ZnO nanowires. The supply of vacuum in the pneumatic line made the PDMS membrane bend up, enabling the gene delivered algal cells to be recovered from the outlet of the microchannel. We successfully confirmed Hyg3 gene integrated in microalgae by amplifying the inserted gene through polymerase chain reaction (PCR) and DNA sequencing. The efficiency of the gene delivery to algal cells using the ZnO nanowire-incorporated microdevice was 6.52×10^4 - and 9.66×10^4 -fold higher than that of a traditional glass bead beating and electroporation.

KEYWORDS: ZnO nanowire, microalgal, gene delivery, transformation, high throughput, microfluidics, biofuel



INTRODUCTION

The depletion of fossil fuels pushes human beings to search for next generation energy resources. Among a variety of energy resources, biomass based bioenergy production recently garnered great attention, and in particular, microalgae driven biodiesel generation looks promising due to its convenience for large scale cultivation, its potentials to create a variety of biobased commodity products besides lipid, and an ecofriendly carbon circulation. Thus, current research has been focused on the development of superior species of microalgae which show high lipid content and rapid growth rate.

Typical cellular transformation has been well established in the fields of recombinant microorganism, protein expression, and cancer therapy.^{1–3} For example, genetically engineered *Escherichia coli* and cyanobacteria can produce valuable chemical products such as biofuels.^{4–6} In this context, many efforts have also been dedicated to transforming microalgal cells to retain the aforementioned desired properties.⁷ In the process of the cellular transformation in microalgae, the first step is to

deliver the target gene into the cells. For this purpose, a traditional glass bead beating or an electroporation method has been widely utilized. However, the current state of the art technology shows very low target gene delivery and gene expression efficiency due to the thick algal cell membrane, and the transfer of the exogenous DNA into microalgae mainly depends on the random diffusion of targets, which does not guarantee quantitative gene delivery.^{8–11} Moreover, the exogenous DNA or other biomolecules may be damaged during the glass bead beating or an electroporation, leading to inaccurate and undesired gene integrity in the nucleus.⁸ To overcome such limitations of the conventional methods, new type gene delivery platforms have been proposed which displayed low cell viability degradation and higher exogenous gene delivery performance. A photodegradable polymer based

Received: October 20, 2015

Accepted: November 19, 2015

Published: November 19, 2015

gene carrier system was adapted to demonstrate superior specific gene delivery capability which reduces intranuclear gene transcription barrier.¹² The microalgal cells were encapsulated with the target genes inside the microdroplets and were transformed on the droplet based electroporation.¹³ Recently, biomolecule functionalized nanostructures such as nanoneedles were also used for inserting target biomolecules inside the cells.¹⁴ Moreover, spatially localized and functionalized straightforward silicon nanowires were developed for efficient and diverse transfer of biomolecules into primary mammalian cells. The facile surface modification and the punctuation ability of the sharp tip allow the nanowire to be applied for the biomolecule delivery into the cytoplasm in cells.¹⁵ Depending on the target molecule and cell types, physical properties of nanowires such as top morphology, diameter, and sharpness could be manipulated.¹⁶

However, the previously reported methods hold significant limitations in terms of cellular manipulation. They simply relied on the gravitational force for the cells to settle down on the functionalized nanowires, which resulted in low efficiency and low controllability of target gene delivery. In addition, the detachment of the target delivered cells from the nanowire was carried out by treatment of trypsin that can change the cellular state morphologically and functionally. Thus, a nonchemical cellular manipulation method would be ideal to control cellular movement toward the nanowire array and cell recovery from the nanowire array with minimal damage for further downstream applications.

In this study, we report a novel gene delivery platform for microalgal transformation by combining the nanowire array and the pneumatic actuated microvalve system. As a model, Hyg3 gene was coated on the ZnO nanowires through a disulfide based linker and directly penetrated into the *Chlamydomonas reinhardtii* (*C. reinhardtii*) by a microvalve actuation in a high throughput manner. The compression by a pneumatic microvalve allows the *C. reinhardtii* to be penetrated into the ZnO nanowires, and the gene delivered *C. reinhardtii* was recovered by supplying vacuum in the pneumatic line.

■ EXPERIMENTAL SECTION

Culture Conditions. Green microalgal *C. reinhardtii* were incubated and subcultured as follows. A single *C. reinhardtii* colony was picked on the trisacetate phosphate (TAP) agar plate and inoculated into a 75 mL filter cap cell culture flask with 10 mL of a TAP culture medium. The seed culture of an algal cell suspension was centrifuged at 2500g for 2 min and was washed with 1 mL of a fresh TAP medium again. *C. reinhardtii* was resuspended with 10 mL of a TAP culture medium and incubated under 120 $\mu\text{mol photons m}^{-2} \text{s}^{-1}$ in a 120 rpm shaking incubator at 23 °C. *C. reinhardtii* were grown until they reached a density of 1.02×10^7 cells mL^{-1} in a TAP medium.

Hyg3 Gene Preparation. The Hyg3 amplicons, harboring hygromycin B resistance gene *aph7^r*, which was fused with *rbcs2* intron 1 of *Chlamydomonas*, were prepared using pHyg3 as a template.⁸ The resultant Hyg3 amplicons consisted of $\beta 2$ -tubulin gene promoter (TUB2), aminoglycoside phosphotransferase gene (*aph7^r*), and 3' untranslated regions of *rbcs2* (Supporting Information Figure S1 and Table S1). Target Hyg3 gene amplification was conducted using a DreamTaq Green PCR Master Mix (2X) (Thermo Scientific, Waltham, MA, USA) with a forward primer (5'-HS-GCC GAG CAT ACA ACA CAC CT-3') and a reverse primer (5'-CGC TTC AAA TAC GCC CAG-3') (Integrated DNA Technologies, Coralville, IA, USA). A 270 μL aliquot of 0.5 mM dithiothreitol (DTT) was mixed with 30 μL of the Hyg3 PCR products for 2 h under gentle vortexing to remove the protecting group, producing a

thiol modified Hyg3 gene. The DTT treated amplicons were purified by an AccuPrep PCR purification kit (Bioneer, Daejeon, Republic of Korea), and 180 μL of the purified Hyg3 PCR products was mixed with 320 μL of 1 \times phosphate buffer saline (PBS) for the downstream experiments.

Synthesis of ZnO Nanowires. The Hyg3 ZnO nanowires were synthesized by a typical hydrothermal method.¹⁷ A precursor solution was synthesized with zinc nitrate hexahydrate ($\text{Zn}(\text{NO}_3)_2 \cdot 6\text{H}_2\text{O}$, 98%; Sigma-Aldrich), hexamethylene tetramine (HMTA, $\text{C}_6\text{H}_{12}\text{N}_4$, 99+%; Sigma-Aldrich), and PEI ($(\text{C}_2\text{H}_5\text{N})_n$, Sigma-Aldrich) in deionized (DI) water. A substrate coated with ZnO seeds was immersed in the ZnO precursor solution and heated to 95 °C. After 2.5 h, the ZnO nanowire grown substrate was washed with DI water and air-dried. The bottom glass wafer was masked except the trench part, and a thin ZnO layer on the microfluidic channel was formed by a radiofrequency (RF) sputtering method (150 W, 3 min). The thickness of a seed layer was about 10 nm. The glass substrate with a seed layer was immersed in a precursor solution and heated at 95 °C for 2.5 h. The average diameter and height of the resultant ZnO nanowires were 36.8 and 529.5 nm, respectively. Since the density of the ZnO nanowires on the glass substrate was 300 nanowires μm^{-2} , the number of ZnO nanowires on the area of 3 cm of length \times 500 μm of width was approximately 4.5×10^9 .

Gene Functionalization on ZnO Nanowires. A 0.2 mM amount of PDPA (3-(2-pyridylthio)propanoic acid) solution was injected from the inlet to the ZnO nanowire-incorporated microfluidic channel for 2 h to coat ZnO nanowires with the PDPA moieties. Then, 500 μL of a thiol functionalized Hyg3 gene solution (1.53 $\text{ng } \mu\text{L}^{-1}$) was introduced into the microfluidic channel and incubated for 8 h for a covalent chemical linkage of the Hyg3 gene with the PDPA linker through disulfide exchange reaction.

Fabrication of the Microfluidic Device. The microchannel whose dimension was 3 cm of length \times 500 μm of width \times 35 μm of depth was fabricated via a wet etching method. First, an amorphous Si (200 nm of thickness) was deposited on a 4 in. glass wafer by plasma enhanced chemical vapor deposition (PECVD). S1818G positive photoresist was spin coated on the amorphous Si coated glass wafer, and UV light was exposed to form a microchannel pattern. AZ 300 MFI developer (AZ Electronics Materials, Singapore) was used to develop the S1818G photoresist pattern and the exposed Si was removed by a SF_6 reactive ion etching (RIE). Then, the exposed glass wafer was further etched by a HF solution to form 35 μm of a channel depth. The residual photoresist was removed by acetone, and the amorphous Si was then eliminated in a 5 M KOH solution. The top glass manifold layer was also fabricated based on the conventional photolithography process similar to that of the microchannel. The bottom glass microfluidic channel layer, a PDMS membrane, and a glass manifold layer were treated using an O_2 plasma cleaner for 1 min 30 s for permanent bonding. Both the inlet and outlet holes (1 mm of diameter) of the PDMS membrane were manually punched by unirec punch device (Harris, Melbourne, FL, USA).

Cultivation of Transformed *C. reinhardtii*. Hyg3 gene delivered *C. reinhardtii* were recovered in the ZnO nanowire-incorporated microdevice by adding 300 μL of a TAP culture medium into the microfluidic channel. The obtained transformed microalgal cells were autofluoresced by a laser scanning confocal microscope using 650 nm long path wavelength and EZ-C1 software (Nikon, Tokyo, Japan) to visualize *in vivo* chlorophyll of *C. reinhardtii*. Prior to the addition of hygromycin B in the cultivation, the recovered gene transformed *C. reinhardtii* were stabilized for 18 h without light exposure, which could recover the physical damage on the cell membrane induced by the ZnO nanowires. To verify the Hyg3 gene integrity in *C. reinhardtii*, 300 μL of the algal cell suspension was cultured in a TAP medium with 0, 2, 5, and 10 $\mu\text{g mL}^{-1}$ hygromycin B, and the cellular proliferation was monitored every day for 2 weeks.

Cultivation on an Agar Plate. To evaluate the transformation efficiency using the ZnO nanowire-incorporated microdevice, the gene delivered microalgae were recovered and cultured on the TAP agar plate which contained 10 $\mu\text{g mL}^{-1}$ hygromycin B. A 100 μL aliquot of the transformed *C. reinhardtii* solution, which was cultured in a TAP

medium containing 0, 2, 5, and 10 $\mu\text{g mL}^{-1}$ hygromycin B, was mixed with 3 mL of a TOP agar (TAP + 0.5% agar) and spread onto the TAP agar plate for transformant selection. After 2 weeks, the formed single colonies of Hyg3 gene integrated *C. reinhardtii* were counted.

Integrated Hyg3 Identification by PCR. The transformed *C. reinhardtii* grew until their density reached 8.25×10^6 cells mL^{-1} . A 50 μL aliquot of the Hyg3 gene inserted *C. reinhardtii* solution was taken, and the genomic DNA of *C. reinhardtii* was extracted with i-genomic BYF DNA Extraction Mini Kit (iNtRON Biotechnology). A 2 μL aliquot of the genomic DNA solution was used as a PCR template. Two sets of the primers were designed to amplify the Hyg3 gene. The amplicon of 844 bp was produced by the forward primer (5'-TCT CGT TGG GGC ATG-3') and the reverse primer (5'-TCA ACG AGC GCC TCC ATT-3'), while the amplicon of 1,620 bp was generated by the forward primer (5'-GAA GGT CGT TTT CCA TCC-3') and the reverse primer (5'-CAA CCA ACA AAA TTG CAA AAC-3'). PCR thermal cycling was executed using a DreamTaq Green PCR Master Mix (Life Technology) according to the following protocol: an initial denaturation at 95 $^{\circ}\text{C}$ for 5 min, 35 PCR cycles of 95 $^{\circ}\text{C}$ for 1 min, 60 $^{\circ}\text{C}$ for 30 s, and 72 $^{\circ}\text{C}$ for 1 min 35 s, and a final extension step at 72 $^{\circ}\text{C}$ for 5 min. The resultant Hyg3 gene amplicons were analyzed on the gel electrophoresis using 1% of an EB agarose gel (LPS solution).

RESULTS AND DISCUSSION

Structure of the ZnO Nanowire-Incorporated Microdevice. Figure 1A shows the schematics of the nanowire-

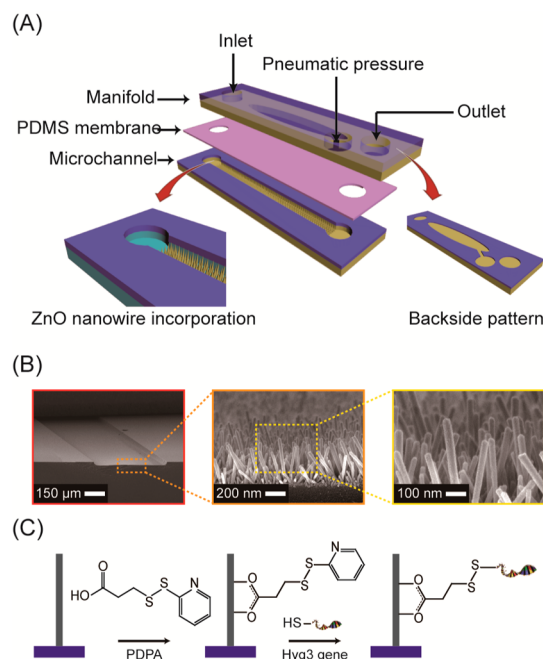


Figure 1. (A) Schematics of the ZnO nanowire-incorporated microfluidic device. (B) Scanning electron microscope images of the synthesized ZnO nanowires on the bottom glass layer. (C) Functionalization process of ZnO nanowires with the target genes by a covalent disulfide exchange reaction.

incorporated microdevice. It consists of three layers: from top to bottom, a glass manifold, a monolithic PDMS membrane, and a ZnO nanowire embedded microfluidic channel. A glass manifold has a pneumatic control line, and inlet and outlet holes from which a cell solution was injected and recovered. A PDMS membrane has also two holes which were aligned with the inlet and outlet holes of a glass manifold. After O_2 plasma treatment, the PDMS membrane was sandwiched between the

two glass layers. A digital image of the assembled microdevice is shown in Supporting Information Figure S2. ZnO nanowires were grown in the trench of the bottom glass layer. The straight one-dimensional microchannel was fabricated by a wet etching photolithographic process with a dimension of 35 μm of depth \times 500 μm of width \times 3 cm of length (Figure 1A). On the bottom of the microfluidic channel, ZnO nanowires were synthesized by a hydrothermal method. Briefly, crystalline seeds were deposited on the glass substrate and precursors were aggregated on the seed which resulted in rapid growth on the (001) polar plane of ZnO nanowires. Meanwhile, polyethylenimine (PEI) surfactants stabilized the ZnO nanowire surface to prevent lateral growth.¹⁸ In this work, hexamethylenetetramine (HMTA) worked as a capping agent to inhibit the horizontal growth of the ZnO nanowire, which resulted in the nanowires with high aspect ratio.¹⁷ Synthesized ZnO nanowires have strong mechanical properties such as a high Young's modulus (\sim 140 GPa) and strength (\sim 7 GPa). A small diameter of ZnO nanowires would be ideal considering the low cellular damage during penetration. Thus, the seed was prepared by a sputtering process, which could produce ZnO nanowires with approximately 36.8 nm of diameter that can lead to reasonable cellular viability. The angle of the prepared ZnO nanowires was a little bit variable, but most of the ZnO nanowires were almost vertical with an angle of 79.1 $^{\circ}$ (standard deviation, 7.0 $^{\circ}$) that could penetrate the cell membrane (Figure 1B). The length of the ZnO nanowire fabricated inside the microfluidic channel was about 529.5 nm on average.

Functionalization on ZnO Nanowires. As-synthesized ZnO nanowires in the microchannel were functionalized with the Hyg3 gene as shown in Figure 1C. First, the Hyg3 gene was amplified by PCR using a thiol modified forward primer. The resultant thiol modified amplicons were deprotected by incubation with 0.5 mM of dithiothreitol (DTT) for 2 h and purified by a PCR purification kit (Bioneer) to remove the excess of DTT. A 30 μL aliquot of thiol modified Hyg3 amplicon solution was obtained with a concentration of 9.42 ng μL^{-1} . On the other hand, ZnO nanowires were treated with 0.2 mM PDDPA to functionalize the nanowire surface via covalent bonding with a carboxylate group. The pyridyl moiety in the PDDPA linker is a good leaving group during the disulfide exchange reaction. Thus, the thiol modified Hyg3 gene was incubated with the functionalized nanowires for 8 h to react with the PDDPA linker and was finally connected with ZnO nanowires by disulfide bond.

Operation of the Microfluidic Device. As described in Figure 1A, the ZnO nanowire-incorporated microfluidic device consisted of a glass manifold, flexible PDMS membrane, and ZnO nanowire embedded microchannel substrate. To demonstrate the high performance of the gene delivery to the microalgal cells using the proposed microdevice, we chose *C. reinhardtii* as a model which has been well studied in terms of the physiological behavior and molecular genetic engineering.^{19–21} A stock solution of *C. reinhardtii* (1.02×10^7 cells mL^{-1}) was injected from the inlet to the bottom microchannel, and ca. 1.84×10^4 cells were loaded in the trench whose volume was 525 nL. Then, the nanowire mediated Hyg3 delivery was performed. The entire process of the gene delivery in the microdevice was composed of four steps: injection, pressurization, washing, and recovery.

Figure 2 shows a flowchart for the perspective view of the microdevice according to the pneumatic operation. First, *C. reinhardtii* suspended in the TAP culture medium were loaded

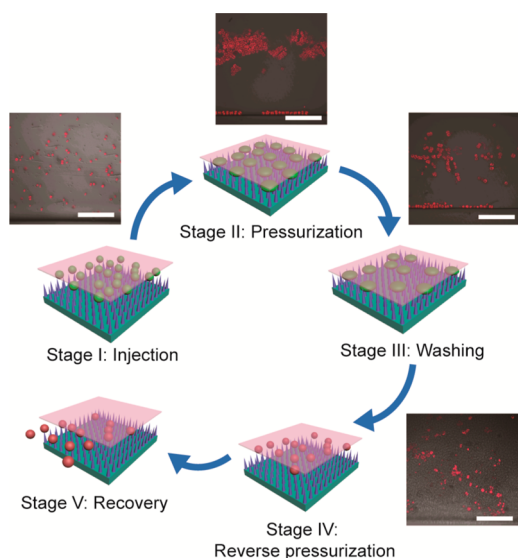


Figure 2. Illustration of the working principle of the pressure driven target gene delivery in the microdevice. (Inset: Autofluorescence images of *in vivo* chlorophyll of *C. reinhardtii* during the injection, pressurization, washing, and reverse pressurization step. Scale bar: 50 μm .)

in the ZnO nanowire embedded microchannel (stage I) and pressed down toward the nanowires upon the supply of air in the pneumatic line. During this step, cells were penetrated by the gene coated nanowires and stuck to the bottom microchannel (stage II). The introduction of the TAP culture medium flushed out the floating microalgal cells, while the penetrated cells were held in position due to the compression of the upper PDMS membrane (stage III). The incubation allows the coated Hyg3 gene to be transferred into cells by the reduction of disulfide bond. The disulfide bond which bridges between the Hyg3 gene and ZnO nanowires can be cleaved owing to the reducing environments of algal cells. Once the gene delivery was complete, vacuum was applied in the pneumatic line to exert back pressure, so that *C. reinhardtii* were detached from the nanowire array (stage IV). The detached cells were recovered from the outlet by injecting the medium solution in the inlet hole (stage V).

A series of digital micrographs of Figure 2 show the variation of the cellular morphology for each step. We could observe cells as red due to the autofluorescence of chlorophyll *in vivo*. In a clockwise direction, the microscope images revealed the injected floating cells, the pressurized cells, the attached cells after a washing step, and the detached cells.

Through the whole process, five different types of pressure were applied to verify a relationship between the effect of a pneumatic compression on a degree of algal cell transfection and its cell viability. The ZnO nanowire punctuated algal cells under no pressure (as a control experiment) and 144, 344, 564, and 900 mbar of PDMS compression from the microdevice were incubated for 18 h to get a cellular stabilization. In Supporting Information Figure S3, as the stronger pressure has been applied, the more distinctive green fluorescence of FAM in algal cells has also been observed which means a greater amount of exogenous DNA is delivered into the algal cells (55.50, 58.53, 108.30, 142.76, and 140.74 au). The viability of algal cells, however, has been suddenly decreased at 900 mbar pressure condition which can be recognized by a dramatic increase in blue fluorescence of trypan blue (Thermo Fisher

Scientific, Pittsburgh, PA, USA) stained algal cells in the bottom fluorescence images of Supporting Information Figure S3, which means critical damage on algal cell viability. Moreover, attributed to the significant algal cell viability reduction at 900 mbar of pressurization, there is a saturation point of green fluorescence in algal cells and, therefore, we have chosen 564 mbar of pressure in the following experiments to achieve high algal cell viability and exogenous DNA delivery performance on the green algal cell.

When *C. reinhardtii* were flattened by the pneumatic pressurization between the PDMS membrane and ZnO nanowire array, the diameter of the algal cells increased from 8.33 to 10.33 μm . A 1.25-fold increment in the size indicated that cells were pressed down and directly contacted with the gene coated nanowires. The washing process removed the unpunctuated cells, leaving only the attached cells in the nanowire array. Upon pneumatic vacuum supply, *C. reinhardtii* were released and recovered their original size (8.37 μm), suggesting that the 36.8 nm diameter of the ZnO nanowires did not cause significant cell disruption during the target gene delivery process (Figure 3A). An additional cellular viability

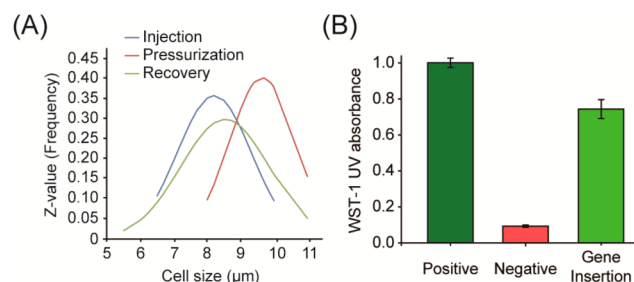


Figure 3. (A) Size distribution of *C. reinhardtii* during the injection, pressurization, and recovery step. Algal cell size was transformed into a normal distribution. (B) Cell viability test using a WST-1 cell proliferation assay.

confirmation of the recovered algal cells at 564 mbar of pressurization was analyzed by a premix cell proliferation assay WST-1 kit (TAKARA Bio Inc., Shiga, Japan). We compared the cell viability of nanowire punctuated cells with that of a positive control, which directly used the cultured microalgae for WST-1 assay. Figure 3B shows that *C. reinhardtii* penetrated by ZnO nanowires represented 74.3% cell viability of a positive control. Although there was some damage on the cell membrane, such an issue would be overcome by tuning the nanowire density.

Evaluation of the DNA Delivery to the Cells via ZnO Nanowires. To assess the DNA delivery efficiency by the proposed nanowire-incorporated microdevice, we immobilized the fluorescein (FAM) and thiol labeled single stranded DNAs (FAM labeled ssDNA) (5'-FAM-AATTGGCCAATTGGCC-SH-3') on the ZnO nanowire (Supporting Information Figure S4) and then performed DNA transfer to the microalgae following the same scheme of Figure 2. A certain concentration of a FAM labeled ssDNA solution (10^{-3} , 10^{-2} , 10^{-1} , 1, 2, 5, and 10 μM) was injected to functionalize the ZnO nanowire array and measured the initial fluorescence intensity of the ZnO nanowire per area of $36 \mu\text{m} \times 36 \mu\text{m}$. After the FAM labeled DNA delivery to the cells, we measured the fluorescence intensity of the ZnO nanowire again. By comparing the fluorescence intensity before and after DNA delivery, we could estimate the DNA delivery efficiency by the ZnO nanowire-incorporated microdevice.

Figure 4A shows the microscope images of a single algal cell after the FAM labeled ssDNA delivery. Not only the red

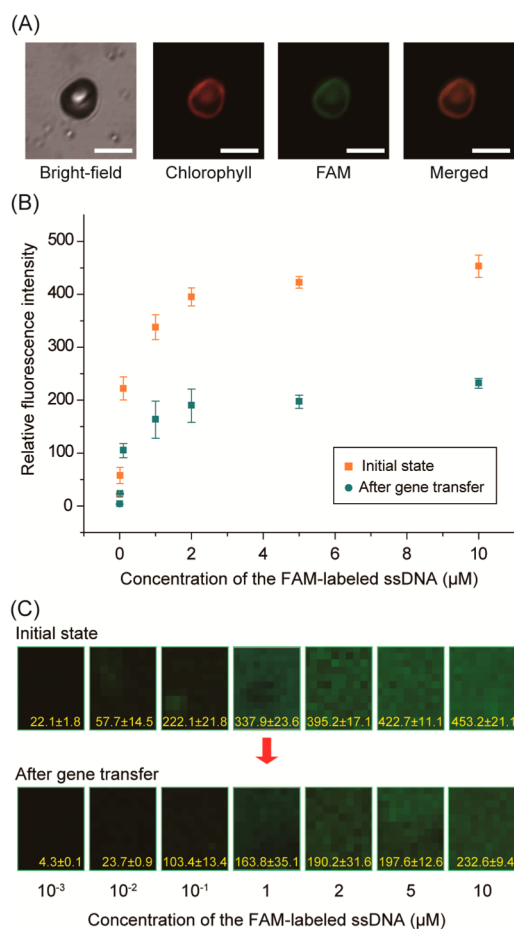


Figure 4. (A) Fluorescence images of the single *C. reinhardtii* after injection of the FAM labeled ssDNA. From left to right, the bright field image, the red fluorescence of the *in vivo* chlorophyll, the green fluorescence of the transferred FAM labeled ssDNA, and the merged image of *C. reinhardtii*. Scale bar: 10 μm. (B) Fluorescence intensity on the ZnO nanowire array before and after exogenous DNA delivery at various concentrations of injected FAM labeled ssDNA. (C) Comparison of confocal fluorescence images on the nanowire substrate before and after FAM labeled ssDNA delivery into *C. reinhardtii*.

fluorescence signal which is derived from *in vivo* chlorophyll but also the green signal that comes from the FAM were observed, demonstrating a success of the FAM labeled ssDNA transfer into microalgal cell. We have calculated the efficiency of the FAM labeled DNA transfer based on the relative fluorescence intensity reduction at a specific rectangular area (1,296 μm²) of the ZnO nanowire substrate. Supporting Information Table S2 shows the relative fluorescent intensity before and after the exogenous DNA delivery into *C. reinhardtii* depending on the injected DNA concentration, and the transfer efficiency was measured by dividing the fluorescence intensity subtraction by the initial fluorescence intensity. The fluorescence intensity on the ZnO nanowire array at the initial state was 22.1, 57.7, 222.1, 337.9, 395.2, 422.7, and 453.2 at the concentrations of 10⁻³, 10⁻², 10⁻¹, 1, 2, 5, and 10 μM, respectively. The fluorescence intensities on the ZnO nanowire array after DNA delivery were 4.3, 23.7, 105.4, 163.8, 190.2, 197.6, and 232.6. Thus, the

approximate DNA delivery efficiencies into microalgae were 0.75, 0.61, 0.53, 0.52, 0.52, 0.53, and 0.49, respectively. These data were plotted in Figure 4B. It seems that the DNA binding sites may be saturated from the injected DNA concentration of 2 μM, while the average transfer efficiency retained nearly 52%. Figure 4C shows the fluorescence images before and after FAM labeled DNA delivery according to the concentration of the FAM labeled ssDNA solution. Obviously, we could observe the reduction of the fluorescence intensity after DNA delivery into the algal cells. The fluorescence intensity variation on the surface of ZnO nanowires allows us to estimate the relative amount of delivered DNA into green algal cell, *C. reinhardtii*. These results imply that a qualitative target gene delivery comparison would be possible by manipulating the concentration of exogenous DNA functionalized on the ZnO nanowires and measuring the fluorescence intensity reduction on the nanowire surface before and after exogenous DNA delivery.

Growth Analysis of Microalgae. To confirm successful integration of Hyg3 gene, the recovered transformed *C. reinhardtii* was cultured with addition of hygromycin B (0, 2, 5, and 10 μg mL⁻¹). Figure 5A shows the fluorescence images of the proliferated *C. reinhardtii*. The growth trend of Hyg3 gene integrated *C. reinhardtii* was varied depending on the concentration of hygromycin B. Without addition of hygromycin B (a control experiment), transformed *C. reinhardtii* represented an explosive population increase (the first row). On the other hand, the growth rate with hygromycin B was reduced compared with the control experiment, and the higher concentration of the hygromycin B caused the lower growth rate of the algal cells (from the second to the fourth row). We performed the identical cell culture experiment using wild type *C. reinhardtii* for comparison. Panels B and C of Figure 5 display the cell concentration versus incubation time using wild type and transformed *C. reinhardtii*, respectively. As expected, wild type could grow only without hygromycin B. Even 2 μg mL⁻¹ hygromycin B inhibited the cellular proliferation (Figure 5B). On the contrary, transformed *C. reinhardtii* revealed different growth profiles depending on the concentration of hygromycin B. The proliferation profile of transformed *C. reinhardtii* without hygromycin B was similar to that of wild type, but the cell concentration (1.2 × 10⁷ cells mL⁻¹) was less than the wild type (3.5 × 10⁷ cells mL⁻¹) by ca. 3-fold. These results indicated that transformed *C. reinhardtii* still retained high viability, but slight physical damage would be unavoidable. Under the conditions of 2 and 5 μg mL⁻¹ hygromycin B, algal cells displayed slow growth rate, and ca. 82-fold and 17-fold increases in the cell number over the initial number were produced after 14 days. The 10 μg mL⁻¹ hygromycin B, however, prohibited the cell proliferation. Thus, Hyg3 gene transformed *C. reinhardtii* via the nanowire mediated technique were dependent on the antibiotics concentration for cellular growth and could survive below 5 μg mL⁻¹ hygromycin B.

We further investigated the Hyg3 gene integration in the cells by using the PCR and DNA sequencing. The cultured cells with antibiotics in the presence of 5 μg mL⁻¹ hygromycin B were collected, and the genomic DNA was extracted to be used as a template in the PCR. We designed the two primer sets which could amplify the integrated Hyg3 gene with 844 bp and 1,620 bp. Figure 6 shows the resultant gel electropherogram in which 844 bp as well as 1,620 bp Hyg3 gene bands appeared clearly, while there was no Hyg3 band for nontransformed *C. reinhardtii* cells. The 844 bp and 1,620 bp PCR amplicons were

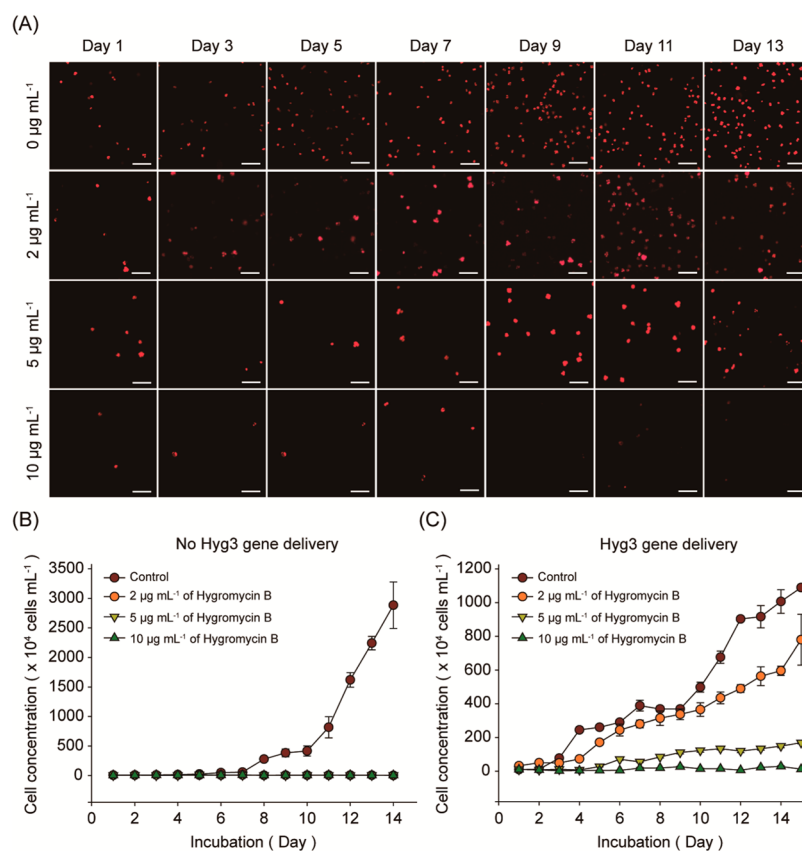


Figure 5. (A) Images of the algal cell proliferation up to 13 days. *C. reinhardtii* were cultivated in the presence of hygromycin B (0, 2, 5, and 10 µg mL⁻¹), and the autofluorescence of *in vivo* chlorophyll of *C. reinhardtii* was monitored. Scale bar: 50 µm. (B) Growth profiles of the nontransformed *C. reinhardtii* with addition of 0, 2, 5, and 10 µg mL⁻¹ hygromycin B. (C) Growth profiles of the transformed *C. reinhardtii* with addition of 0, 2, 5, and 10 µg mL⁻¹ hygromycin B.

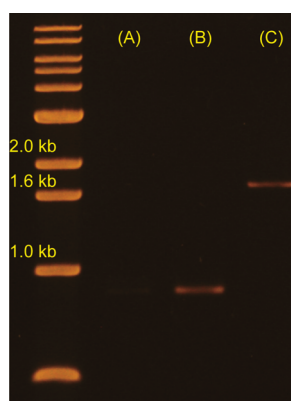


Figure 6. Gel electrophoresis of the Hyg3 PCR products using (A) wild type *C. reinhardtii*, (B) transformed *C. reinhardtii* (844 bp amplicon), and (C) transformed *C. reinhardtii* (1,620 bp).

sequenced, and the sequencing data were matched with target gene sequence (Supporting Information Figures S5 and S6). These results clearly demonstrated that the Hyg3 gene was successfully inserted into *C. reinhardtii* and there was no degradation of exogenous target genes during the transformation.

Transformation Efficiency. The exogenous gene expression level is not absolutely proportional to the number of inserted target genes because of a DNA degradation problem and a random combination of the exogenous gene with the microalgal genome. The accurate and controllable nanowire

mediated gene delivery would enhance such a transformation efficiency compared with the conventional methods. To evaluate the transformation efficiency, we loaded the microalgal cells (1.84×10^4) in the microchannel for Hyg3 gene delivery and then recovered them for cultivation on the TAP agar plate which contained 10 µg mL⁻¹ hygromycin B. Based on the number of the formed single colony on the TAP agar plate which was *ca.* 120, the transformation efficiency of ZnO nanowire-incorporated microdevice was calculated as 6.52×10^{-3} . The transformation efficiencies of the glass bead beating and the electroporation method were 1.00×10^{-7} and 6.73×10^{-8} , respectively.^{8,13} Therefore, the ZnO nanowire assisted gene transformation efficiency shows 6.52×10^4 - and 9.66×10^4 -fold enhancements in the conventional algal cell transformation performance (Table 1).

Moreover, a typical bead beating method could scratch the microalgal cells or even rupture them, so the microalgae cannot maintain their original cell viability, and the exogenous genes can be fragmented. Similarly, the conventional electroporation

Table 1. Comparison of the Microalgal Transformation Efficiency

methods	no. of cells used per transformation	no. of produced colonies
ZnO nanowire	1.84×10^4	120
glass bead beating	3.00×10^8	30.0
electroporation	1.57×10^7	1.06

method, which employs electric pulses, may easily hinder microalgal cells survival due to high electric intensity.²² Since the typical algal cell transformation actually depends on random diffusion of exogenous gene into the cells, the exact gene delivery capability into the nucleus would be diminished. On the other hand, the ZnO mediated target gene transfer method enables the direct penetration of ZnO nanowires into the algal cell membrane, and successful gene insertion into the microalgal cells in a controllable way, so that the DNA degradation could be minimized and direct gene transfer to the nucleus would be more feasible, thereby enhancing the transformation efficiency.

CONCLUSION

In summary, we demonstrated a high throughput ZnO nanowire assisted gene delivery microfluidic device for microalgal cell transformation. Besides the nanowire fabrication, the microfluidic device was equipped with the pneumatic PDMS microvalve so that the cellular manipulation for attachment and detachment from the ZnO nanowire array could be manageable. As a proof of concept, the Hyg3 gene was coated on the surface of ZnO nanowires and delivered to *C. reinhardtii* to be transformed into a hygromycin B resistant strain. The transformed *C. reinhardtii* could be cultured in the presence of hygromycin B, meaning that the exogenous gene integration was successful. We further identified the integrated Hyg3 gene by the PCR and DNA sequencing. In comparison to the conventional glass bead beating and electroporation method, the proposed ZnO nanowire-incorporated microdevice showed superior transformation efficiencies by 6.52×10^4 - and 9.66×10^4 -fold, respectively. Thus, our novel methodology can provide an important tool to improve the transformation efficiency, which is critical to generating superior transformed microalgae for biofuel production.

ASSOCIATED CONTENT

Supporting Information

The Supporting Information is available free of charge on the ACS Publications website at DOI: 10.1021/acsami.5b09964.

Vector map of pHyg3, digital image of the integrated microdevice, verification of the fluorescence DNA delivery performance of microdevice and algal cell viability assay under five different types of PDMS compression condition, schematics for covalent chemical bonding of the fluorescence DNA onto ZnO nanowires, sequencing data for the identification of the inserted Hyg3 gene amplicon (844 and 1,620 bp), sequence of Hyg3 gene cassette (amplicon), and comparison of the fluorescent intensity of the ZnO nanowire array before and after delivery of the FAM labeled ssDNA into the microalgae (PDF)

AUTHOR INFORMATION

Corresponding Author

*Tel.: +82-42-350-3973. Fax: +82-42-350-3910. E-mail: seots@kaist.ac.kr.

Notes

The authors declare no competing financial interest.

ACKNOWLEDGMENTS

This work was supported by the Korea CCS R&D Center (KCRC) grant funded by the Korea government (Ministry of

Science, ICT & Future Planning; 2014M1A8A1049278) and the Engineering Research Center of Excellence Program of Korea Ministry of Science, ICT & Future Planning (MSIP)/National Research Foundation of Korea (NRF; 2014R1A5A1009799).

REFERENCES

- (1) Akiyama, H.; Okuhata, H.; Onizuka, T.; Kanai, S.; Hirano, M.; Tanaka, S.; Sasaki, K.; Miyasaka, H. Antibiotics-free stable polyhydroxyalkanoate (PHA) production from carbon dioxide by recombinant cyanobacteria. *Bioresour. Technol.* **2011**, *102* (23), 11039–11042.
- (2) Assenberg, R.; Wan, P. T.; Geisse, S.; Mayr, L. M. Advances in recombinant protein expression for use in pharmaceutical research. *Curr. Opin. Struct. Biol.* **2013**, *23* (3), 393–402.
- (3) Weldon, J. E.; Pastan, I. A guide to taming a toxin – recombinant immunotoxins constructed from *Pseudomonas* exotoxin A for the treatment of cancer. *FEBS J.* **2011**, *278* (23), 4683–4700.
- (4) Na, D.; Yoo, S. M.; Chung, H.; Park, H.; Park, J. H.; Lee, S. Y. Metabolic engineering of *Escherichia coli* using synthetic small regulatory RNAs. *Nat. Biotechnol.* **2013**, *31* (2), 170–174.
- (5) Choi, Y. J.; Lee, S. Y. Microbial production of short-chain alkanes. *Nature* **2013**, *502*, 571–574.
- (6) Parmar, A.; Singh, N. K.; Pandey, A.; Gnansounou, E.; Madamwar, D. Cyanobacteria and microalgae: A positive prospect for biofuels. *Bioresour. Technol.* **2011**, *102* (22), 10163–10172.
- (7) Parker, M. S.; Mock, T.; Armbrust, E. V. Genomic insights into marine microalgae. *Annu. Rev. Genet.* **2008**, *42*, 619–645.
- (8) Berthold, P.; Schmitt, R.; Mages, W. An Engineered *Streptomyces hygroscopicus aph 7'* Gene Mediates Dominant Resistance against Hygromycin B in *Chlamydomonas reinhardtii*. *Protist* **2002**, *153* (4), 401–412.
- (9) Bigelow, T. A.; Xu, J.; Stessman, D. J.; Yao, L.; Spalding, M. H.; Wang, T. Lysis of *Chlamydomonas reinhardtii* by high-intensity focused ultrasound as a function of exposure time. *Ultrason. Sonochem.* **2014**, *21* (3), 1258–1264.
- (10) Ciudad, G.; Rubilar, O.; Azócar, L.; Toro, C.; Cea, M.; Torres, Á.; Ribera, A.; Navia, R. Performance of an enzymatic extract in *Botryococcus braunii* cell wall disruption. *J. Biosci. Bioeng.* **2014**, *117* (1), 75–80.
- (11) Yamano, T.; Iguchi, H.; Fukuzawa, H. Rapid transformation of *Chlamydomonas reinhardtii* without cell-wall removal. *J. Biosci. Bioeng.* **2013**, *115* (6), 691–694.
- (12) Lee, H.; Kim, Y.; Schweickert, P. G.; Konieczny, S. F.; Won, Y.-Y. A photo-degradable gene delivery system for enhanced nuclear gene transcription. *Biomaterials* **2014**, *35* (3), 1040–1049.
- (13) Qu, B.; Eu, Y.-J.; Jeong, W.-J.; Kim, D.-P. Droplet electroporation in microfluidics for efficient cell transformation with or without cell wall removal. *Lab Chip* **2012**, *12* (21), 4483–4488.
- (14) Peer, E.; Artzy-Schnirman, A.; Gepstein, L.; Sivan, U. Hollow Nanoneedle Array and Its Utilization for Repeated Administration of Biomolecules to the Same Cells. *ACS Nano* **2012**, *6* (6), 4940–4946.
- (15) Shalek, A. K.; Robinson, J. T.; Karp, E. S.; Lee, J. S.; Ahn, D.-R.; Yoon, M.-H.; Sutton, A.; Jorgolli, M.; Gertner, R. S.; Gujral, T. S.; MacBeath, G.; Yang, E. G.; Park, H. Vertical silicon nanowires as a universal platform for delivering biomolecules into living cells. *Proc. Natl. Acad. Sci. U. S. A.* **2010**, *107* (5), 1870–1875.
- (16) Kim, J.; Hong, J. W.; Kim, D. P.; Shin, J. H.; Park, I. Nanowire-integrated microfluidic devices for facile and reagent-free mechanical cell lysis. *Lab Chip* **2012**, *12* (16), 2914–2921.
- (17) Sugunan, A.; Warad, H.; Boman, M.; Dutta, J. Zinc oxide nanowires in chemical bath on seeded substrates: Role of hexamine. *J. Sol-Gel Sci. Technol.* **2006**, *39* (1), 49–56.
- (18) Greene, L. E.; Yuhas, B. D.; Law, M.; Zitoun, D.; Yang, P. Solution-Grown Zinc Oxide Nanowires. *Inorg. Chem.* **2006**, *45* (19), 7535–7543.
- (19) Staut, M.; Cuiné, S.; Cagnon, C.; Fessler, B.; Nguyen, M.; Carrier, P.; Beyly, A.; Beisson, F.; Triantaphylidès, C.; Li-Beisson, Y.;

Peltier, G. Oil accumulation in the model green alga *Chlamydomonas reinhardtii*: Characterization, variability between common laboratory strains and relationship with starch reserves. *BMC Biotechnol.* **2011**, *11* (1), 7.

(20) Bae, S.; Kim, C. W.; Choi, J. S.; Yang, J.-W.; Seo, T. S. An integrated microfluidic device for the high-throughput screening of microalgal cell culture conditions that induce high growth rate and lipid content. *Anal. Bioanal. Chem.* **2013**, *405* (29), 9365–9374.

(21) Msanne, J.; Xu, D.; Konda, A. R.; Casas-Mollano, J. A.; Awada, T.; Cahoon, E. B.; Cerutti, H. Metabolic and gene expression changes triggered by nitrogen deprivation in the photoautotrophically grown microalgae *Chlamydomonas reinhardtii* and *Coccomyxa* sp. C-169. *Phytochemistry* **2012**, *75* (0), 50–59.

(22) Brown, L. E.; Sprecher, S.; Keller, L. Introduction of exogenous DNA into *Chlamydomonas reinhardtii* by electroporation. *Mol. Cell. Biol.* **1991**, *11* (4), 2328–2332.